On the influence of suspended sediment transport on the generation of offshore sand waves

Fenneke van der Meer[1], Suzanne J.M.H. Hulscher[1] and Joris van den Berg[2]

[1] Water Engineering and Management, University of Twente, Enschede, The Netherlands F.M.vanderMeer@utwente.nl
[2] Numerical Analysis and Computational Mechanics, University of Twente, Enschede, The Netherlands.

Summary. Sand waves are bed-forms occurring in shallow seas. Although their characteristics are mainly affected by bed load transport, during rough weather suspended sediment transport can influence their characteristics. As a first step to model these influences, we added suspended sediment transport to a numerical 2DV model that was specifically developed for simulating sand waves. In this paper, results are presented for initial, small amplitude, sand waves. Incorporating suspended sediment transport increases the growth rate of sand waves significantly while their wave length is more robust. Furthermore, we found that the results are sensitive to flow conditions, as expected, and sediment diffusivity, which needs a more advanced description.

1 Introduction

The sea bed of a shallow sea is rarely flat. Various bed-forms occur, varying from small scale ripples and mega-ripples to large scale sand banks. Sand waves are bed-forms with a scale between these two extremes. The wavelengths of these bed-forms vary between 100 and 800 meters, and heights can reach up to one third of the water depth (i.e. a maximum of around 10 meters in 30 meters of water). These characteristics, together with the fact that sand waves can migrate several meters per year and that they cover the majority of the Southern North Sea ([16], Figure 1, mean that they affect human activities in shallow seas. Therefore, we aim to model and so better understand the dynamics of these sand waves and the influence of both the tidal motion and weather conditions.
Observations indicate that sand waves change due to suspended sediment transport, especially during rough weather conditions. For example, [11] investigated sand waves in the Dutch coastal area, together with their physical environment. He concluded that sand waves occur under sufficiently high cur-

Bernard J. Geurts et al. (eds), Particle Laden Flow: From Geophysical to Kolmogorov Scales, 29–41.

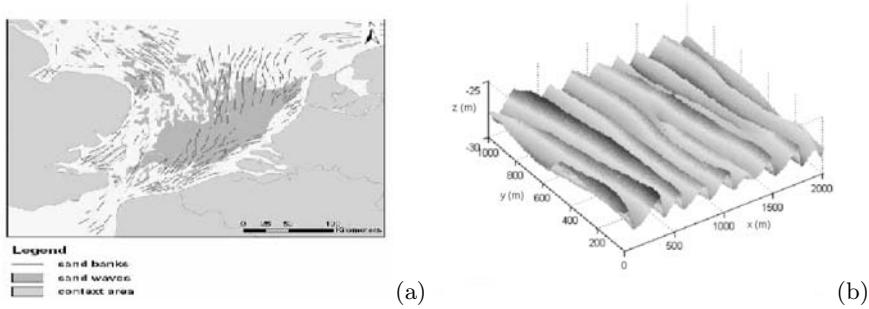

Fig. 1. (a) Sand wave and sand bank occurrence in the Southern part of the North Sea; (b) measured field data of a sand wave field in the North Sea.

rent velocities, low to moderate wave activity and an asymmetry in the tidal ellipse. Observations indicated that sand waves were lower on locations with more suspended sediment transport. Recently, [13] investigated weather influences on compound sand waves and mega-ripples. Although mega-ripples were found to be directly influenced by an individual storm, [13] concluded that sand wave morphology is a result of the general wind-wave climate. This, together with the local setting in which sand waves occur, was reasoned to lead to variation in sand wave shapes.

Offshore in shallow seas, bed load transport is expected to be the main sediment transport mechanism. As the water depth is in the order of tens of meters, under normal conditions short surface waves rarely interact with the sea bed. As grain sizes in sand wave areas are typically around the 200-300μm, vertical velocity due to the tidal current is lower than the fall velocity for the sediment for most of the tide, so the suspension of sediment only occurs during part of the tidal cycle. However, under storm conditions, suspended sediment can play an important role, especially in relatively shallow water. [2] found that under normal conditions and a flat bed, suspended sediment transport could be 30% of the bed load transport. [4] found seasonal dependency of sand wave height and migration in the Marsdiep. In this long term data set (1998-2005), sand waves were on average 30% higher after calm summer periods and lower after winter seasons. This variability was greater in locations where, due to finer sediment and stronger tidal currents, suspended sediment is more abundant.

Though techniques to measure sand wave characteristics as height and migration are improved over the past decades, still measurements are expensive and little detailed data is available. Modeling sand wave characteristics improves our knowledge of sand wave behavior and the processes underlying this behavior. In this way modeling can help where data is unavailable or insufficient.

The described studies indicate that suspended sediment transport influences sand waves, yet the effects have not yet been thoroughly investigated. Though

the occurrence of suspended sediment transport increases the total sediment transport, it is not clear beforehand, whether suspended sediment will increase the sand wave growth, or will repress this growth. This depends on the distribution of erosion and deposition of the suspended sediment over the sand wave.
In this paper, we aim to contribute to an understanding of the effects of suspended sediment transport on the initial stage of sand wave formation. Hereto, we investigated the effect of implementing suspended sediment transport in the 2DV numerical sand wave code and the sensitivity of several parameters. After a short state of the art overview (Section 2.1), we will discuss the used model and the equations implemented to describe suspended sediment (Section 3). In Section 4, the simulations and their results are described, after which in Section 5 the results are discussed and conclusions are drawn.

2 Sand wave modeling

2.1 State of the art

[8] described sand waves as free instabilities of the coupled system of a sandy sea bed and a tidal flow. In such a system, vertical vortices play a crucial role. Small perturbations of the sea floor cause small perturbations in the flow field and vice versa. The bed can be either stable, which means that disturbances will be damped, or unstable, which means that bed perturbations will grow and the sea bed is changed. When perturbations are unstable (i.e. triggering growth) the flow field is changed such that, averaged over the tidal cycle, small vertical rest circulation cells occur (Figure 2). These cells cause small net transport to the crests of the perturbation, thereby causing growth. This process can be described using a linear stability analysis. A linear analysis is valid only for small, formally only infinitesimal small, amplitude perturbations. To overcome this limitation, numerical tools have been developed that allow the simulation of fully developed sand waves ([12],[15]). [12] showed that non-linear sand waves can be simulated with only bed load transport and an unidirectional steady current. [1] investigated the effects of tidal waves and asymmetry, explaining migration of small linear sand waves. [15] extended to fields of sand waves and showed sand waves to develop from random small bottom disturbances. Recently [3] showed effects of wind and waves on a sand pit situation, in which waves had a quantitative but no qualitative effect on the sand pit. In these studies, the effects of suspended sediment on sand wave formation, i.e. the aim of this paper, have not yet been studied.

3 Sand wave model

The simulation method used in this paper is based on the model described by [8], who applied a linear stability analysis. The linear stability analysis predicts

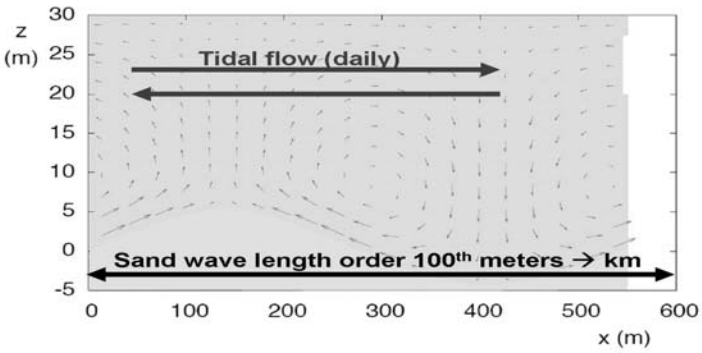

Fig. 2. Averaged over a tidal cycle, vertical circulations cells can occur due to small perturbations in the sea floor, causing growth or decay of these perturbations.

sand waves to grow exponentially in their initial stage. Starting with a small sinusoidal perturbation of the sea floor, characterized by a certain wavelength, growth or decay of the particular perturbation can be predicted numerical as well. For an initial bed with the form $h = A\sin(\frac{2\pi}{L}x)$, with A being the amplitude and L the wavelength of the sand wave, the growth rate can be determined by the change in the sand wave height using $\omega = \frac{1}{\partial t}\log(\frac{h_{new}}{h_{old}})$. The growth rate is expressed in 1/s. When the growth in height corresponding to various wave lengths is known, the wave length that induces the fastest growth in height can be found (fastest growing mode, FGM). The FGM indicates the dominant sand wavelength that is expected to be the most likely to occur in reality as it grows fastest in height.

We start the simulation by prescribing sinusoidal, small amplitude, bed waves. The tidal flow is modeled as a symmetrical sinusoidal current prescribed by means of a forcing. Using the bathymetry, a tidal flow is calculated. Since the flow changes over a time-scale of hours and the morphology over a time-scale of years, the bathymetry is expected to be invariant over a single tidal cycle. Once the tidal flow is known, the bed changes are calculated over this typical tide, using sediment transport equations. This is repeated until the bed evolution exceeds a certain value, after which a new tidal flow is calculated. This, in turn, affects the bed and so the process is iterative. In this way, we are able to simulate the morphological time scale accurately, while avoiding long computation times.

The model consists of the hydrostatic flow equations for 2DV flow (Equations 1 and 2). In the horizontal direction, periodic boundary conditions are used. For model details, we refer to [15].

$$\frac{\partial u}{\partial x} + \frac{\partial w}{\partial z} = 0 \tag{1}$$

$$\frac{\partial u}{\partial t} + u\frac{\partial u}{\partial x} + w\frac{\partial w}{\partial z} = -g\frac{\partial \zeta}{\partial x} + \frac{\partial}{\partial z}\left(A_v \frac{\partial u}{\partial z}\right) \tag{2}$$

In these equations x, z represent the horizontal and vertical directions and u and w the horizontal and vertical flow velocities. The variable t denotes time, ζ is the water surface elevation, g is the constant of gravity and A_v is the constant eddy viscosity.
Boundary conditions at the bed disallow flow through the bottom (equation 3). Further, a partial slip condition compensates for the constant eddy viscosity, which overestimates the eddy viscosity near the bed (equation 3). The parameter S denotes the amount of slip, with $S = 0$ indicating perfect slip and $S = \infty$ indicating no slip. At the water surface, there is no friction and no flow through the surface (equations 4).

$$w - u\frac{\partial h}{\partial x} = 0|_{seabed} \quad ; \quad A_v \frac{\partial u}{\partial z} = Su|_{seabed} \tag{3}$$

$$\frac{\partial u}{\partial z} = 0|_{surface} \quad ; \quad w = \frac{\partial \zeta}{\partial t} + u\frac{\partial \zeta}{\partial x}|_{surface} \tag{4}$$

The flow and the sea bed are coupled through the continuity of sediment (equation 5). Sediment is transported in two ways: as bed load transport (q_b) and as suspended load transport (q_s), which are modeled separately. Here we use a bed load formulation after [9] (equation 6).

$$\frac{\partial h}{\partial t} = -\left(\frac{\partial q_b}{\partial x} + \frac{\partial q_s}{\partial x}\right) \tag{5}$$

$$q_b = \alpha |\tau_b|^b \left[\frac{\tau_b}{|\tau_b|} - \lambda \frac{\partial h}{\partial x}\right] \tag{6}$$

Grain size and porosity are included in the proportionality constant α, τ_b is the shear stress at the bottom, h is the bottom elevation with respect to the spatially mean depth H and the constant λ compensates for the effects of slope on the sediment transport. For more details, we refer to [9] or [18].
In order to model suspended sediment transport q_s, we describe sediment concentration c throughout the water column, i.e. a 2DV model. Horizontal diffusion is assumed to be negligible in comparison with the other horizontal influences. The vertical flow velocity, w, is smaller than the fall velocity for sediment, w_s, and can be neglected in this equation, leading to equation (7). This means that the sediment is suspended only by diffusion from the bed boundary condition (equation 12). As the flow velocity profile is already calculated throughout the vertical direction, suspended sediment transport q_s can be calculated using equation (8).

$$\frac{\partial c}{\partial t} + u\frac{\partial c}{\partial x} = w_s \frac{\partial c}{\partial z} + \frac{\partial}{\partial z}\left(\epsilon_s \frac{\partial c}{\partial z}\right) \tag{7}$$

$$q_s = \int_a^H u(z)c(z)dz \tag{8}$$

$$w_s = \frac{\nu D_*^3}{18 D_{50}} \tag{9}$$

$$D_* \equiv \left(\frac{g(s-1)}{\nu^2}\right)^{1/3} D_{50} \tag{10}$$

$$\epsilon_s = A_v \tag{11}$$

The parameter ϵ_s denotes the vertical diffusion coefficient (here taken equal to A_v), a is a reference level above the bed above which suspended sediment occurs, D is the grain size. The dimensionless grain size is denoted by D_*, $(s-1)$ is the relative density of sediment in water ($\frac{\rho_s - \rho_w}{\rho_w}$), with ρ_w the density of water and ρ_s the density of the sediment and ν is the kinematic viscosity. Equations (9-11) are due to [18].
Suspended load is defined as sediment which has been entrained into the flow. By definition, it can only occur above a certain level above the sea bed. At this reference height, a reference concentration can be imposed as a boundary condition. Various reference levels and concentrations exist for rivers, near-shore and laboratory conditions. Those often applied are [17, 14, 5, 21]. For offshore sand waves, the choice of a reference height is more difficult than it is for the shallower (laboratory) test cases. In this case, the reference equation of [17] (equation 12) is used, with a reference height of 1 percent of the water depth, corresponding with the minimum reference height proposed in [17].

$$c_a = 0.015 \frac{D}{0.01 H D_*^{0.3}} \left(\frac{|\tau| - \tau_{cr}}{\tau_{cr}}\right)^{1.5} \tag{12}$$

The reference concentration at height a above the bed is given by c_a and τ_{cr} is the critical shear stress necessary to move sediment.
Both the gradient and the quantity of suspended sediment are largest close to the reference height. Therefore, concentration values are calculated on a grid with a quadratic point distribution on the vertical axis, such that more points are located closer to the reference height and fewer points are present higher in the water column. To complete the set of boundary conditions for sediment concentration, we disallow flux through the water surface.

4 Model results

In this paper, we concentrate fully on the influence of suspended sediment on the initial state of sand waves. We started each simulation with a sinusoidal bed-form with an amplitude of 0.1m.

Next, we investigated the (initial) growth rate and the fastest growing sand wavelength (FGM). Table 1 shows some basic values used in the simulations

and the characteristics of the simulations are given in Table 2. Where possible, typical values for sand waves in the North Sea are used. Note that $\bar{u}$ is defined as the depth-averaged maximum flow velocity.

Table 1. Parameter values for the reference simulation

parameter	value	unit	parameter	value	unit
$\bar{u}$	1	m/s	ϵ_v	0.03	m^2/s
H	30	m	D	300	μm
A_v	0.03	m^2/s	w_s	0.025	m/s
S	0.01	m/s	a	0.3	m
α	0.3	-			

Table 2. Simulations

simulation	bed load	suspended load	varied parameter	simulation	bed load	suspended load	varied parameter
reference	√	-	-	3	√	√	ϵ_v
1	√	√	-	4	√	√	u
2	√	√	ref. height a	5	√	-	u

4.1 transport simulations

Figure 3(a) shows the growth rate for different sand waves lengths simulated in the reference simulation. Moreover, the figure shows that the FGM is approximately 640m. For simulation 1, we included suspended sediment in the reference computation. Figure 3(b) shows a comparison between the reference simulation and simulation 1. The growth rate is shown for a range of wavelengths. Most remarkable is the increase of the growth rate by a factor of approximately 10. This was unexpected as suspended sediment is assumed to be of minor importance in these circumstances. The FGM for simulation 1 is 560m, 80m less than in the reference simulation.

In figure 4, the concentration profile in the water column at a crest point over the tidal period is shown (upper figure), compared with the flow velocities (lower figure). The sediment is only entrained into the first few meters of the water column. The sediment concentration follows the flow without an apparent lag, as the flow velocity near the bed is small and slowly changes over time. However, these small variations in velocity are enough for the suspended sediment to be entrained and to settle again within one tidal cycle. Close to the reference height, the maximum sediment concentration is around $3{\cdot}10^{-4}$ m^3/m^3 (0.8 kg/m^3).

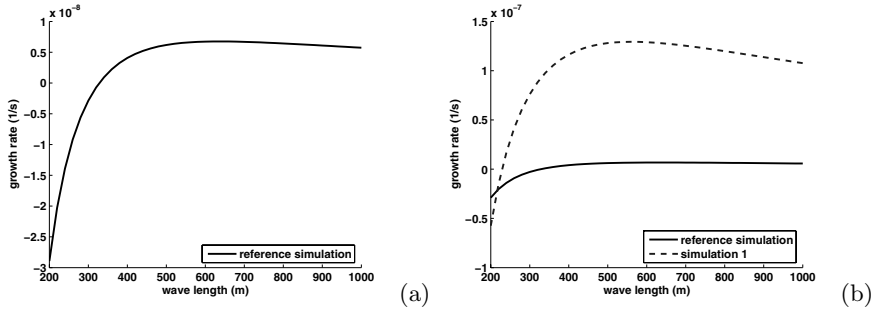

Fig. 3. (a) Growth rate – reference simulation; (b) growth rate – simulation 1 (solid), compared with reference simulation (dashed). Parameters in Table 1.

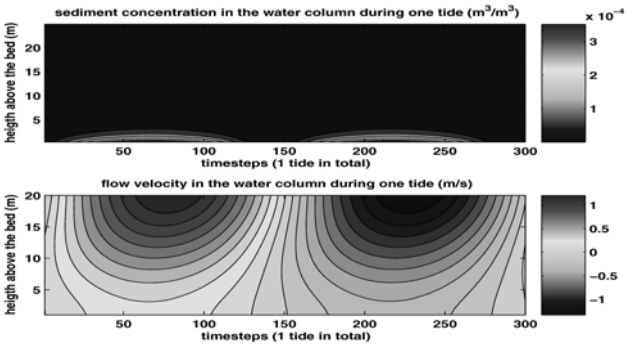

Fig. 4. Sediment concentration (upper) and flow velocity (lower) on one location over a tidal period, for simulation 1. More details see Fig 6 (upper).

4.2 sensitivity simulations

To study the influence of the reference height on the sediment entrainment and suspended transport, the reference height in simulation 2 equation (12) is

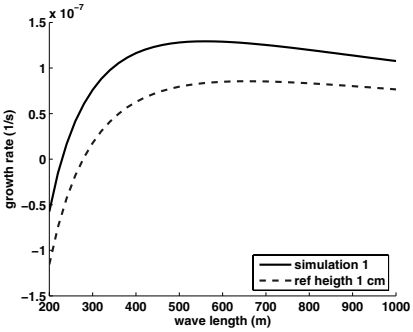

Fig. 5. Growth rate for simulation 2 (solid), compared to simulation 1 (dashed). For simulation characteristics, see Table 1.

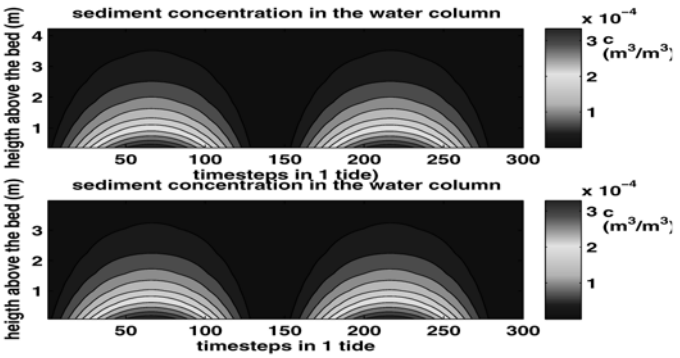

Fig. 6. Sediment concentration in the first 4 meters above a certain point of the sand wave during one tide. Comparison between simulation 1 (upper) and 2 (lower)

decreased to 0.01m above the bed. This height is used as the lowest measurable height for suspended sediment in shallow seas ([10, 6]). The results are shown in figures 5 and 6. It can be seen in figure 5 that the growth rate decreases for a lower reference height, whereas the FGM becomes 660m. Note that the growth rate, compared to the situation without suspended sediment, is still larger. In figure 6, it can be seen that, for the first 4 meters above the reference height, no change occurs, except that the sediment is entrained about 0.30m higher in the reference simulation. This difference is a direct result of the change in reference height itself (from 0.30m to 0.01m). Therefore the difference in growth rate is solely due to the contribution of these 0.29m to the integration of $u \cdot c$ over the water column.

Table 3. Simulation results, for varied values the first (second) value is for the +50% (-50%) simulation

simulation	FGM (m)	growth rate for FGM (1/s)	simulation	FGM (m)	growth rate for FGM (1/s)
reference	640	6.75e-9	3	860 - 350	1.24e-7 - 1.12e-7
1	560	1.29e-7	4	810 - 340	2.40e-7 - 3.87e-8
2	660	8.55e-8	5	670 - 610	1.23e-8 - 2.20e-9

In simulations 3 and 4, a sensitivity analysis was carried out for the diffusion coefficient and the flow velocity. The value of sediment diffusivity, ϵ_v, in the reference situation was assumed to be equal to the eddy viscosity Av, though its value is not established. Both ϵ_v and $\bar{u}$ were varied by $\pm$ 50% of their reference values. Their influence on the growth rate ω and the FGM are shown in figures 7(a) and 7(b). It can be seen that the FGM increases significantly for increasing ϵ_v (FGM becomes 860m), and decreases for decreasing ϵ_v (FGM

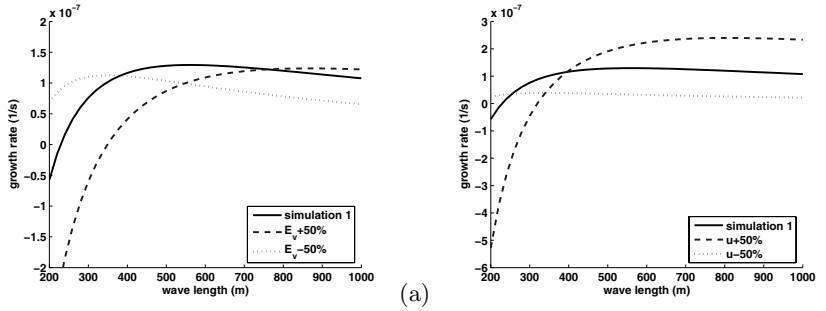

Fig. 7. (a) Growth rate for simulation 3, variable ϵ_v; simulation 1 (solid), ϵ_v+50% (dashed), ϵ_v-50% (dotted). (b)Growth rate for simulation 4, variable $\bar{u}$; simulation 1 (solid), $\bar{u}$+50% (dashed), $\bar{u}$-50% (dotted).

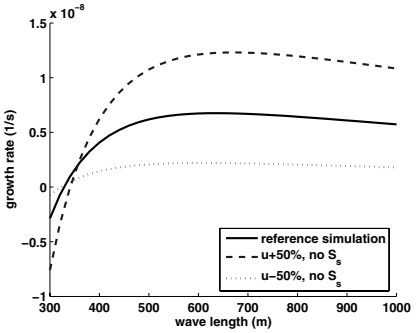

Fig. 8. Growth rate for simulation 5, variable $\bar{u}$ and no q_s; reference (solid), $\bar{u}$+50% (dashed), $\bar{u}$-50% (dotted)

becomes 350m). The growth rate of the FGM remains of the same order of magnitude. However, smaller wavelengths are damped more severely for increasing sediment diffusivity.

For the flow velocity $\bar{u}$, the FGM again tends to increase with increasing $\bar{u}$ and vice-versa (for values, see Table 3), and smaller wavelengths are damped more for higher values of $\bar{u}$. For the growth rate, we now see a different effect. As expected from the nonlinear $\bar{u}$ in the sediment transport equation, the growth rate is highly affected by $\bar{u}$. The higher the value of $\bar{u}$, the higher the initial growth rate for the FGM.

As shown in figure 7(b), suspended sediment transport increases the effect of variation in $\bar{u}$. If we compare this influence to the influence of varying $\bar{u}$ without suspended sediment transport (figure 8) it is clear that suspended sediment increases the effect of changing velocities on the FGM (45% change instead of 5% change in sand wavelength, for varying $\bar{u}\pm$50%). For the growth rate of the FGM, this influence is less pronounced; the decrease (increase) of

growth rate with higher(lower) $\bar{u}$ is 82% (67%) for the case without suspended sediment and 86% (70%) for the case with suspended sediment.

5 Discussion and conclusions

In the reference simulation, ϵ_v is assumed to be equal to the value of A_v. Various coupling equations exist to relate ϵ_v to A_v, varying from ϵ_v being larger than to being smaller than A_v. [2] therefore assumed ϵ_v equal to A_v, as no generally accepted method is available. Figure 7(a) shows that varying the value of ϵ_v influences the FGM significantly, though the growth rate itself is hardly influenced. Possibly the large difference in growth rates between the case with and without suspended load transport (reference simulation and simulation 1) is caused, not by the value of ϵ_v, but by the constant value of both the eddy viscosity and sediment diffusivity. Due to these constant values, A_v might be overestimated near the bed, which is corrected for by the partial slip boundary condition. Such a correction is not used for the ϵ_v, possibly leading to an increase of suspended sediment. Due to the constant ϵ_v this sediment can also be entrained higher into the water column.
Unfortunately, little field data for offshore sediment transport is available at the moment, hindering a direct comparison with the results. [6] measured suspended sediment offshore in the North Sea at a water depth of 13 meters. Only during minor storms suspended sediment was detected. Maximal values were around 2.3 kg/m^3 for 0.3m above the bed and 0.2 kg/m^3 for 1m above the bed. For simulation 1, these values were 8 kg/m^3 and 0.34 kg/m^3. [7] measured sediment concentrations during a severe storm in the North Sea close to the coast of the UK. They found, even under conditions of storm, finer sediment ($\sim$100μm) and a 25m water depth, that the sediment concentration had decreased by about three orders of magnitude after 1 meter ($\pm$ 40 kg/m^3 to 0.03 kg/m^3). However, in the simulations this decrease was slower, leading to higher concentrations higher in the water column ($\pm$ 8 kg/m^3 close to the reference height to 0.03 kg/m^3 at 3 meter above the bed). Although the sediment concentration predicted in the model seems to be in a comparable order of magnitude, transport rates are too large. The most likely cause is the high entrainment of sediment into the water column. Further study on this topic, and the effect of a depth dependent ϵ_v is currently investigated.
As w turned out to be around an order of magnitude smaller then w_s during most of the tide, this term was neglected in the sediment continuity equation (equation 7). However, for higher flow velocities or smaller grain sizes this term will become more important. In that case w should be incorporated and might increase the amount of suspended sediment during a part of the tidal cycle on certain locations on the sand waves, leading to further growth or decay of the sand waves. The effect depends on the specific locations (i.e. crests or troughs) were suspended sediment will erode or deposit.

[17] proposed a reference height for suspension with a minimum value of 1% of the water depth. However, [19] stated that this leads to unrealistically high reference levels in water depths of tens of meters. [19] therefore proposed to use a reference height of 0.01m instead. [10] and [6] also used this height as the lowest measurable height for suspended sediment in shallow seas. Both heights are tested in simulations 1 and 2. They turn out to differ only in the lowest part of the water column, which was excluded from the 1% (i.e. 0.3m) reference height and included in the 0.01m alternative. Thus, the reference height does not change the processes, but only includes or excludes the sediment in the first view centimeters above the bed.
Based on grain sizes, [11] expected suspended transport for grains smaller than 230-300μm. Grains smaller than 170μm would be transported in suspension only, in this case sand waves are rarely found. Recently, [20] showed that a mixture of grain sizes leads to grain size sorting over sand waves, but hardly affects the sand wave form and growth rate in the numerical code. Therefore, in this paper we assumed grains of only one grain size, corresponding with the medium grain size typically found on sand wave fields.

Concluding, the inclusion of suspended sediment transport in a sand wave model demonstrates significant influences of suspended load on the initial growth of sand waves. The influence of various parameters was investigated, showing that the reference height for suspended sediment is of minor importance, while the sediment diffusivity, ϵ_v, and especially the depth averaged maximum flow velocity, $\bar{u}$, largely influence both the FGM and the initial growth rate. Further research will focus on fully developed sand waves and the effects of wind and storm conditions, validated against field data.

Acknowledgment

This research is supported by the Technology Foundation STW, applied science division of NWO and the technology program of the Ministry of Economic Affairs. The authors are indebted to Jan Ribberink for his suggestions.

References

[1] Besio, G., Blondeaux, P., and Frisina, P. (2003). A note on tidally generated sand waves. J. Fluid Dynamics, 485, 171-190
[2] Blondeaux, P. and Vittori, G. (2005a). Flow and sediment transport induced by tide propagation: 1 the flat bottom case. J. Geoph. Res. - Oceans, 110 (C07020, doi:10.1029/2004JC002532)
[3] Blondeaux, P. and Vittori, G. (2005b). Flow and sediment transport induces by tide propagation:2 the wavy bottom case. J. Geoph. Res. - Oceans, 110 (C08003, doi:10.1029/2004JC002545)
[4] Buijsman,M. C. and Ridderinkhof, H. (2006). The relation between currents and seasonal sand wave variability as observed with ferry-mounted adcp. In: PECS 2006, Astoria, OR-USA

[5] Garcia, M. and Parker, G. (1991). Entrainment of bed sediment into suspension. J. Hydraulic Engg, 117 , 414-435

[6] Grasmeijer, B. T., Dolphin, T., Vincent, C., and Kleinhans, M. G. (2005). Suspended sand concentrations and transports in tidal flow with and without waves. In: Sandpit, Sand transport and morphology of offshore sand mining pits, Van Rijn, L. C., Soulsby, R. L., Hoekstra, P., and Davies, A. G.(eds.), U1-U13. Aqua Publications

[7] Green, M. O., Vincent, C. E., McCave, I. N., Dickson, R. R., Rees, J. M., and Pearson, N. D. (1995). Storm sediment transport: observations from the British North Sea shelf. Continental Shelf Res., 15 (8), 889- 912

[8] Hulscher, S. J. M. H. (1996). Tidal-induced large-scale regular bed form patterns in a three-dimensional shallow water model. J. Geoph. Res., 101, 727-744

[9] Komarova, N. L. and Hulscher, S. J. M. H. (2000). Linear instability mechanisms for sand wave formation. J. Fluid Mech., 413, 219-246

[10] Lee, G. and Dade, W. B. (2004). Examination of reference concentration under waves and currents on the inner shelf. J. Geoph. Res., 109 (C02021, doi:10.1029/2002JC001707)

[11] McCave, I. N. (1971). Sand waves in the North Sea off the coast of Holland. Marine Geology, 10 (3), 199-225

[12] Nemeth, A. A., Hulscher, S. J. M. H., and Van Damme, R. M. J. (2006). Simulating offshore sand waves. Coastal Engineering, 53, 265-275

[13] Passchier, S. and Kleinhans, M. G. (2005). Observations of sand waves, megaripples, and hummocks in the Dutch coastal area and their relation to currents and combined flow conditions. J. Geoph. Res. - Earth Surface, 110 (F04S15, doi:10.1029/2004JF000215)

[14] Smith, J. D. and McLean, S. R. (1977). Spatially averaged flow over a wavy surface. J. Geoph. Res., 12 , 1735-1746

[15] Van den Berg, J. and van Damme, D. (2006). Sand wave simulations on large domains. In: River, Coastal and Estuarine Morphodynamics: RCEM2005 , Parker and Garcia(eds.)

[16] Van der Veen, H. H., Hulscher, S. J. M. H., and Knaapen, M. A. F. (2005). Grain size dependency in the occurence of sand waves. Ocean Dynamics, (DOI 10.1007/s10236-005-0049-7)

[17] Van Rijn, L. C. (1984). Sediment transport, part ii: Suspended load transport. J. Hydraulic Engineering, 11, 1613-1641

[18] Van Rijn, L. C. (1993). Principles of sediment transport in rivers, estuaries and coastal seas, vol. I11. Aqua Publications, Amsterdam

[19] Van Rijn, L. C. and Walstra, D. J. R. (2003). Modelling of sand transport in DELFT3D-ONLINE. WL—Delft Hydraulics, Delft

[20] Wientjes, I. G. M. (2006). Grain size sorting over sand waves. CE&M research report 2006R-004/WEM-005

[21] Zyserman, J. A. and Fredsoe, J. (1994). Data-analysis of bed concentration of suspended sediment. J. Hydraulic Engg, 120, 1021-1042.